# Growth of a Multilayer Garnet Crystal Double-Clad Waveguide Structure by Pulsed Laser Deposition

**T. C. May-Smith*, D. P. Shepherd and R. W. Eason**

*Optoelectronics Research Centre, University of Southampton,*

*Highfield, Southampton, SO17 1BJ, UK.*

We report the growth of a multilayer garnet crystal double-clad waveguide structure by Pulsed Laser Deposition. The structure, grown on a YAG (100) substrate, was fabricated from the sequential deposition of YGG, Nd,Cr:GSGG, YGG and YAG, each layer being about 1 micron in thickness. X-ray diffraction analysis has shown that the layers all grew in the epitaxial (100) orientation and energy dispersive X-ray analysis has revealed that the layer compositions are close to those of the target materials. The success of this trial fabrication is an indication of the capability of PLD to produce designer multilayer planar waveguide structures.

Keywords: multilayer, pulsed laser deposition, garnet crystal, optical, waveguide and film.

PACS: 81.15.Fg; 42.70.Hj; 77.55.+f; 68.65.Ac; 42.82.Et

* Author for correspondence: Dr T. C. May-Smith, Optoelectronics Research Centre, University of Southampton, Highfield, Southampton, SO17 1BJ, UK. Tel: +44 (0)23 8059 4531. Fax: +44 (0)23 8059 3149. E-mail: tcms@orc.soton.ac.uk.

## 1. Introduction

A planar waveguide laser pumped by high-power diode arrays should offer an efficient and useful means of brightness enhancement and wavelength manipulation [1]. Multilayer planar waveguide devices analogous to double-clad high-numerical-aperture and large-mode-area optical fibres [2] are highly suitable for this task, as they simultaneously allow the launch of non-diffraction limited pump light and the production of single spatial mode laser output.

The fabrication techniques suitable for creating such devices are currently limited. Liquid Phase Epitaxy (LPE) has been used to create single-clad devices based on YAG ($Y_3Al_5O_{12}$) substrates and cladding layers with a Nd:YAG core [3]. Direct-bonding has been used to create advanced multilayer structures on sapphire substrates with Nd:YAG cores and YAG inner cladding layers capped with a sapphire layer [4]. Although these techniques are both capable of producing high quality crystal layers, they suffer from a relatively slow turnaround compared to PLD, making them undesirable for initial investigations into structure optimisation.

Pulsed Laser Deposition (PLD) is an ideal fabrication technique for multilayer structures and offers several advantages over rival techniques. Preparation and growth is fast, meaning that fabrication time consists mostly of actual deposition, allowing complete multilayer structures to be fabricated in one day. Various targets can be easily obtained as bulk crystal off-cuts and multilayers can be built up by switching between targets in-situ if a multi-target holder is used. The growth of each extra layer

does not introduce any further complications to the fabrication procedure and layer thicknesses can be chosen as required by changing the deposition time or laser repetition rate. The only limitation on materials that can be used is that the crystal structures and compositions are compatible with the requirements for achieving epitaxial growth; there should therefore be small lattice and thermal expansion mismatches across the matrix of materials under consideration.

A significant problem with pumping direct-bonded devices with high powers is that differential thermal expansion can cause the layers to separate [5]. PLD devices should not suffer from this problem because operation at high temperatures when pumping with high powers should lead in fact to relaxation, since the multilayer films are grown at high temperatures (> 800 °C). The use of a multi-target holder also offers the unique opportunity of producing a region of mixed materials between layers. This should offer the significant advantage that there are no distinct layer boundaries that can become weak points as the crystal expands due to high-power operation. Perhaps the only significant disadvantage with PLD is the occurrence of particulates in films which can lead to high losses due to scattering at film interfaces. The use of multilayers however is known to counteract this problem (for cubic materials, such as garnets considered in this paper) by burying particulates and moving the most critical film-air interface further away from where the light is guided [6]. Polishing between layers can also be performed to further reduce the effect of surface-embedded particulates.

The range of garnet crystals available based on elements such as yttrium, gadolinium, aluminium, gallium and scandium provides a versatile basis set of materials for

fabricating multilayer planar waveguides. Garnets make excellent laser host materials because of their wide transparency range, good thermal conductivity and isotropic crystal structure. As can be seen from table 1, each garnet has a slightly different refractive index, making the material system ideally suited to the fabrication of cladding layers. It should also be possible to produce refractive index values between those of the stoichiometric crystals by mixing PLD plumes to produce hybrid crystal layers.

The potential and quality of Nd:GGG films grown by PLD is well proven from previous reports of lasing [25] and losses as low as 0.1 $dBcm^{-1}$ for a 40 μm thick film have been measured [26]. PLD has been used previously for multilayer deposition of superconducting films [27]; although these layers were thinner than the thicknesses desired for double-clad waveguide structures, this serves as an initial proof that layers of multi-component materials can be built up using PLD. The only remaining prerequisite therefore for our desired multilayer fabrication is to show that PLD is capable of sequential growth of several layers of alternating garnet crystal species of order microns in thickness without the quality of the layers suffering during progressive growth.

We have performed such a trial fabrication of multilayers and no apparent deterioration in quality for subsequent layers has been observed. Sequential deposition of YGG ($Y_3Ga_5O_{12}$), Nd,Cr:GSGG ($Nd,Cr:Gd_3Sc_2Ga_3O_{12}$), YGG and YAG was performed on a YAG (100) substrate. To the best of our knowledge, this is the first report of multilayers of different garnet crystal species to be grown by PLD and perhaps also by any other film fabrication technique. As long as stoichiometry has

been preserved for the layers, they should form a double-clad planar waveguide structure consisting of a Nd,Cr:GSGG core, YGG inner cladding layers and YAG outer cladding layers, because the refractive indices of GSGG, YGG and YAG are 1.94, 1.91 and 1.82 respectively [7]. The as-deposited layer thicknesses in our trial run were all between 1.5 and 2.5 microns thick. X-ray diffraction (XRD) analysis has shown that the layers grew as intended in the epitaxial (100) orientation. Energy dispersive X-ray (EDX) analysis has shown that the layer compositions were close to bulk. Scanning electron microscopy (SEM) clearly resolves the separate layer growth due to the slightly different response to incoming electrons of each crystal species.

## 2. Experimental Procedure

A stainless steel vacuum chamber with a base pressure of $10^{-4}$ Pa was used for experiments. For ablation, a 248 nm KrF excimer laser was set to an output of about 175 mJ per pulse (~ 20 ns pulse duration) and was focussed to produce a fluence of about 2.5 $Jcm^{-2}$ at a repetition rate of 10 Hz. Targets were rotated to maximise their usage and the direction of rotation was reversed every 60 seconds. The normal custom for usage of targets is to ablate a few millimeters off the centre of rotation so that a ring is ablated and there is no overlap area. This typically produces an ablated ring of 5 mm in thickness and 15 mm in diameter. The YAG and Nd,Cr:GSGG targets were both single crystal flat discs of sufficient size to enable them to be used in this way. The only YGG target available however was a pellet that had been cut from a single crystal rod of 7 mm in diameter. The limited surface area of this YGG target meant that overlap of the beam was unavoidable as the target rotated and though deposition

was still possible, it is likely that the YGG layers contain a higher frequency of particulates as a result.

Sequential depositions, each of 20 minutes in duration, of YGG, Nd,Cr:GSGG, YGG and YAG were performed to build up the multilayered structure. The vacuum chamber was pumped down to a pressure of $5 \times 10^{-3}$ Pa before each deposition and was subsequently back-filled with oxygen. The flow rate of oxygen was adjusted so that the chamber reached an equilibrium at a pressure of 2.0 Pa for depositions. A YAG (100) substrate of dimensions 10 mm × 10 mm × 1.0 mm was used with one face polished to a high quality finish in preparation for deposition. The substrate was heated by a raster scanned $CO_2$ laser with a wavelength of 10.6 μm. The laser was rastered across the substrate using a grid of 6 × 6 equally spaced points and the time delay between each point was increased slightly at the edges to compensate for the higher rate of emission due to the increased surface area to volume ratio at the edges. A power of 8.0 W was used to obtain a temperature of about 800 °C (this temperature estimate is based on a separate calibration of the heating system involving the melting of small pieces of various high purity metals balanced on top of substrates). The substrate was held in a specially designed alumina cradle to minimise any undesirable heatsinking. A schematic and more detailed description of the apparatus including further standard preparation and fabrication procedures such as pre-deposition ablation and target reconditioning has been reported elsewhere [26]. A more detailed description of the custom-designed heating system has also been reported earlier [28].

XRD analysis was performed with a Siemens D5000 X-ray diffractometer. SEM imaging was performed with a LEO 430 scanning electron microscope and EDX

analysis was performed with an Oxford Instruments ISIS detector that was attached to the LEO 430. The end face of the multilayer structure was polished to produce a clean and smooth surface in preparation for SEM and EDX analysis.

## 3. Results and Discussion

It can be seen from the XRD spectrum shown in figure 1a that only growth in the expected epitaxial (100) orientation has occurred for each layer of different crystal material. It is useful to consider the full-width half-maxima (FWHM) of the XRD peaks because this can give an indication of the crystal quality. Figure 1b shows an expanded view XRD spectrum so that the FWHM of the peaks can be seen clearly; the various properties of the XRD spectrum are summarised in table 2. The *D*-spacing values in table 2 have been normalised using the positions of the YAG substrate peaks.

The normalised *D*-spacing values for the Nd,Cr:GSGG, YGG and YAG capping layer are shifted from database values by ~1.3%, ~0.9% and ~1.0% respectively. This increase in the lattice size of each film compared to bulk is attributed to a small compositional deficiency and is in line with our previous observations of Ga deficiency in single-layer GSGG and YGG films, and Al deficiency in single-layer YAG films. In each case, a deficiency in the ion with the smaller ionic radius (Ga or Al) appears to result in an increased density of lattice sites being occupied by the ion with the larger ionic radius (Gd or Y). The effect of this is to enlarge the crystal structure unit cell dimensions to accommodate the higher density of larger ionic

radius ions. We have found that a similar degree of compositional deficiency can produce a significant amount of strain in thick films (> 40 μm) of Nd:GGG ($Nd:Gd_3Ga_5O_{12}$) grown by the same technique, but none of the deleterious symptoms such as cracking and fragmenting we have witnessed with such thick films have been observed for the multilayer structure discussed here.

The relative peak heights follow a logical order: the YGG layers have led to the most intense diffraction because there are two layers and both are thicker than the other layers; the YAG capping layer followed by the Nd,Cr:GSGG layer have caused the next highest intensity of diffraction because of their relative positions in depth; the YAG substrate has caused the least intense diffraction because it is close to half the maximum penetration depth of X-rays in the structure. The FWHM of (400) film peaks are similar to the FWHM of the YAG substrate (400) peak, indicating that these (400) crystal planes are very well ordered. The (800) film peaks are significantly broader however, suggesting reduced order for these (800) crystal planes.

The garnet crystal structure consists of two distinct alternating crystal planes and one of these is significantly less densely populated with constituent ions. Diffraction from (400) planes always compares self-similar planes and is therefore unaffected by relative disorder between the two different types of planes, whereas diffraction from (800) planes always encompasses all of the crystal structure and is therefore an indication of the total crystal order. The (800) peaks are also expected to be broadened relative to the (400) peaks because a perturbation of an ion by a certain distance (i.e. crystal disorder) will have a worse affect on (800) diffraction than (400) due to the smaller separation of (800) crystal planes.

EDX analysis of the multilayer structure top surface showed that the YAG capping layer was indeed Al deficient as expected from XRD analysis. The relative occurrence of Y and Al was found to be $Y_{3.4 \pm 0.2}Al_{4.6 \pm 0.2}$. The accuracy of this measurement was assessed by analysing a piece of pure YAG target crystal under the same conditions. Oxygen content analysis wasn't possible due to the low energy of the oxygen peak and limitation of the EDX detection. The resolution via EDX analysis is insufficient to resolve the layers separately and a line-scan was performed on the polished end face across the layers instead to give an indication of the respective layer compositions. A graph of the line-scan data is shown in figure 2. There are no clearly defined steps between layers because of this resolution limit. The different layers can however be readily identified and the relative occurrence of the different elements in the layers is as would be expected. Less Al has been found in the capping layer than the substrate. The occurrence of Y is limited to the YAG and YGG layers and the YAG substrate, whereas Sc and Gd are limited to the Nd,Cr:GSGG layer. The occurrence of Ga is higher in the YGG layers than the Nd,Cr:GSGG layer, and is not found in the YAG substrate or YAG layer. The concentrations of Nd and Cr were too small to be detected.

An SEM micrograph of the layers is shown in figure 3, which clearly shows the individual layer contrast. It appears from figure 3 that the YGG layers have grown with a slightly higher deposition rate as these layers are ~50% thicker than the Nd,Cr:GSGG and YAG layers. This suggests that the ablation dynamics of the YGG target were somehow different to the YAG and Nd,Cr:GSGG targets, and could be a

consequence of the compromise made with the relatively small YGG target discussed earlier.

To date, we have not been able to measure overall waveguide loss or performance, or indeed demonstrate laser action via Ti:sapphire pumping for example. The small thicknesses of the layers make launching experiments difficult and it is known that losses tend to be high for PLD films of ~1 μm in thickness; the use of thicker layers with a designed ratio of layer thicknesses will resolve this problem, and we will report our results in this area once new thicker structures have been grown and characterised.

**4. Conclusion**

A double-clad waveguide structure has been fabricated by sequential pulsed laser deposition of YGG, Nd,Cr:GSGG, YGG and YAG on a YAG substrate. The layers, all of around 1 μm in thickness, were found to have grown in the expected epitaxial (100) orientation with a relatively high quality compared to the substrate crystal. Limited resolution EDX analysis revealed that the compositions varied across the layers as would be expected. The layers can be distinguished clearly with SEM imaging. To the best of our knowledge, this is the first report of multilayers (five-layered structures) of different garnet crystal species to be grown by PLD.

This test structure has proven the capability of PLD for fabricating several layers of different garnet crystal without any progressive degradation in film quality occurring as each layer is added. The effect of particulates between film interfaces is important

in such thin structures, and this will be addressed in future growth runs with optimised layer thicknesses.

**Acknowledgements**

The authors would like to acknowledge the support of the Engineering and Physical Sciences Research Council (EPSRC) for funding under Grant No. GR/R74154/01. The authors would also like to acknowledge the services of the NanoMaterials Rapid Prototyping Facility in the School of Physics, University of Southampton, and the EPSRC National Crystallography Service based in the Chemical Crystallography Laboratory at the School of Chemistry, University of Southampton. One of the authors (T. C.M-S) also acknowledges the receipt of an EPSRC studentship.

**References**


[1] D. P. Shepherd, S. J. Hettrick, C. Li, J. I. Mackenzie, R. J. Beach, S. C. Mitchell, H. E. Meissner, J. Phys. D: Appl. Phys. 34 (2001) 2420.

[2] K. Furusawa, A. Malinowski, J. H. V. Price, T. M. Monro, J. K. Sahu, J. Nilsson, D. J. Richardson, Optics Express 9 (2001) 714.

[3] C. L. Bonner, C. T. A. Brown, D. P. Shepherd, W. A. Clarkson, A. C. Tropper, D. C. Hanna, B. Ferrand, Optics Letters 23 (1998) 942.

[4] C. L. Bonner, T. Bhutta, D. P. Shepherd, A. C. Tropper, IEEE J. Quantum Electron. 36 (2000) 236.

[5] J. Wang, J. I. Mackenzie, D. P. Shepherd, CLEO/QELS, Baltimore, USA, May 22-27, 2005, paper CTh16.

[6] S. J. Barrington, T. Bhutta, D. P. Shepherd, R. W. Eason, Opt. Commun. 185 (2000) 145.

[7] R. Adair, L. L. Chase, S. A. Payne, Phys. Rev. B: Condens. Matter Mater. Phys. 39 (1989) 3337.

[8] J. D. Foster, L. M. Osterink, Applied Optics 7 (1968) 2428.

[9] A. Nakatsuka, A. Yoshiasa, T. Yamanaka, Acta Crystallogr., Sect. B: Struct. Sci. 55 (1999) 266.

[10] A. Nakatsuka, A. Yoshiasa, S. Takeno, Acta Crystallogr., Sect. B: Struct. Sci. 51 (1995) 737.

[11] T. H. Allik, C. A. Morrison, J. B. Gruber, M. R. Kokta, Phys. Rev. B: Condens. Matter Mater. Phys. 41 (1990) 21.

[12] Molecular Technology GmbH, Berlin, Germany (crystal supplier). http://www.mt-berlin.com/frames_cryst/descriptions/ysgg.htm. (Last accessed: August 2006).

[13] V. A. Efremov, N. D. Zakharov, G. M. Kuz'micheva, B. V. Mukhin, V. V. Chernyshev, Zhurnal Neorganicheskoi Khimii 38 (1993) 220.

[14] F. Euler, J. A. Bruce, Acta Crystallogr. 19 (1965) 971.

[15] D. L. Wood, K. Nassav, Applied Optics 29 (1990) 3704.

[16] V. B. Gloshkova, Y. V. Zharikov, S. Y. Zinovev, V. A. Krzhizhanovskaya, V. V. Osiko, P. A. Stodenikin, Rep. 289, General Physics Institute, Moscow, 1986.

[17] H. Sawada, J. Solid State Chem. 132 (1997) 302.

[18] C. S. Hoefer, K. W. Kirby, L. G. DeShazer, J. Opt. Soc. Am. B 5 (1988) 2327.

[19] D. S. Sumida, M. S. Mangir, D. A. Rockwell, M. D. Shinn, J. Opt. Soc. Am. B 11 (1994) 2066.

[20] S. Yamazaki, F. Marumo, K. Tanaka, H. Morikawa, N. Kodama, K. Kitamura, Y. Miyazawa. J. Solid State Chem. 108 (1994) 94.

[21] I. P. Kondratyuk, E. V. Zharikov, V. I. Simonov, Kristallografiya 31 (1988) 51.

[22] F. D. Patel, E. C Honea, J. Speth, S. A. Payne, R. Hutcheson, R. Equall, IEEE J. Quantum Electron. 37 (2001) 135.

[23] X. D. Xu, Z. W. Zhao, X. M. He, P. X. Song, G. Q. Zhou, J. Xu, P. Z. Deng, Mater. Lett. 58 (2004) 3153.

[24] B. E. Etschmann, V. A. Strel'tsov, N. Ishizawa, E. N. Maslen, Acta Crystallogr., Sect. B: Struct. Sci. 57 (2001) 136.

[25] C. Grivas, T. C. May-Smith, D. P. Shepherd, R. W. Eason, Opt. Commun. 229 (2004) 355.

[26] T. C. May-Smith, C. Grivas, D. P. Shepherd, R. W. Eason, M. J. F. Healy, Appl. Surf. Sci. 223 (2004) 361.

[27] S. Hontsu, N. Mukai, J. Ishii, T Kawai, S. Kawai, Appl. Phys. Lett. 64 (1994) 779.

[28] S. J. Barrington, R. W. Eason, Rev. Sci. Instrum. 71 (2000) 4223.

**Table and Figure Captions**

Table 1: Various relevant properties of a selection of garnet crystals.

Table 2: Summary of the multilayer structure XRD spectrum properties.

Figure 1a: XRD spectrum of the multilayer structure.

Figure 1b: Expanded detail XRD spectrum of the multilayer structure to show the full-width half-maxima of the peaks.

Figure 2: EDX line-scan of the multilayer structure.

Figure 3: SEM micrograph of the multilayer structure.

| Material | Refractive index (at $\lambda$ = 1.06 μm) | Thermal expansion coefficient ($\times 10^{-6} K^{-1}$) | Lattice constant (Å) | Lattice mismatch to YAG |
|---|---|---|---|---|
| YAG | 1.82 [7] | 6.9 [8] | 12.006 [9] | N/A |
| YGG | 1.91 [7] | [1] | 12.273 [10] | 2.2% |
| YSAG | 1.86 [11] | [17] | 12.271 [11] | 2.2% |
| YSGG | 1.93 [12] | 8.1 [12] | 12.446 [13][2] | 3.7% |
| GAG | [17] | [17] | 12.113 [14] | 0.89% |
| GGG | 1.95 [15] | 8.3 [16] | 12.383 [17] | 3.1% |
| GSAG | 1.89 [18] | 7.7 [19] | 12.389 [20][3] | 3.2% |
| GSGG | 1.94 [7] | 8.0 [16] | 12.544 [21] | 4.5% |
| YbAG | 1.83 [22] | 8.6 [23] | 11.939 [24] | -0.56% |

Table 1

[1] These material parameters remain unknown to us to date.

[2] The closest crystallographic data available was for $Y_3Sc_{1.43}Ga_{3.57}O_{12}$ and this has been used as an approximation of YSGG.

[3] The closest crystallographic data available was for $Gd_{2.91}Sc_{1.80}Al_{3.15}O_{11.80}$ and this has been used as an approximation of GSAG.

| Crystal (orientation) | $2\theta$ (degrees) | FWHM (degrees) | *D*-spacing (Å) | Normalised *D*-spacing (Å) | Database *D*-spacing (Å) |
|---|---|---|---|---|---|
| Nd,Cr:GSGG (400) | 27.982 | 0.07 | 3.186 | 3.179 | 3.1360 [21] |
| Nd,Cr:GSGG (800) | 57.894 | 0.14 | 1.592 | 1.589 | 1.5680 [21] |
| YGG (400) | 28.746 | 0.09 | 3.103 | 3.097 | 3.0682 [10] |
| YGG (800) | 59.573 | 0.17 | 1.551 | 1.548 | 1.5341 [10] |
| YAG (400) | 29.382 | 0.08 | 3.037 | 3.031 | 3.0015 [9] |
| YAG (800) | 60.968 | 0.21 | 1.518 | 1.516 | 1.5008 [9] |
| YAG substrate (400) | 29.700 | 0.05 | 3.006 | - | 3.0015 [9] |
| YAG substrate (800) | 61.723 | 0.06 | 1.502 | - | 1.5008 [9] |

Table 2

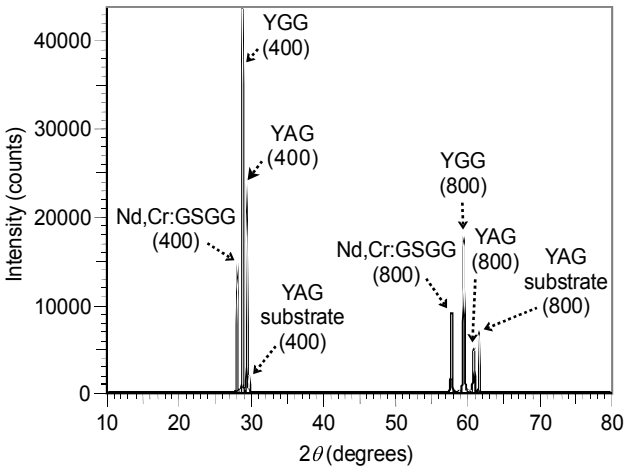
YGG
(400)
YAG
(400)
Nd,Cr:GSGG
(400)
YAG
substrate
(400)
YGG
(800)
YAG
(800)
Nd,Cr:GSGG
(800)
YAG
substrate
(800)
Intensity (counts)
40000
30000
20000
10000
0
10
20
30
40
50
60
70
80
2θ (degrees)

Figure 1a

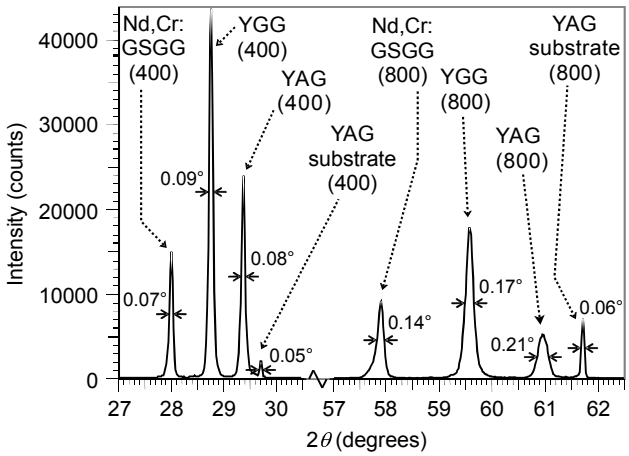
Nd,Cr:
GSGG
(400)
YGG
(400)
YAG
(400)
YAG
substrate
(400)
Nd,Cr:
GSGG
(800)
YGG
(800)
YAG
(800)
YAG
substrate
(800)
0.09°
0.08°
0.07°
0.05°
0.14°
0.17°
0.21°
0.06°
Intensity (counts)
40000
30000
20000
10000
0
27
28
29
30
57
58
59
60
61
62
2θ (degrees)

Figure 1b

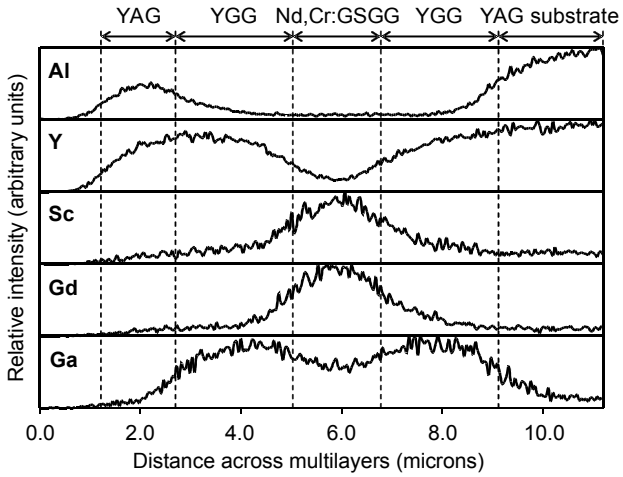
YAG
YGG
Nd,Cr:GSGG
YGG
YAG substrate
Al
Y
Sc
Gd
Ga
Relative intensity (arbitrary units)
0.0
2.0
4.0
6.0
8.0
10.0
Distance across multilayers (microns)

Figure 2

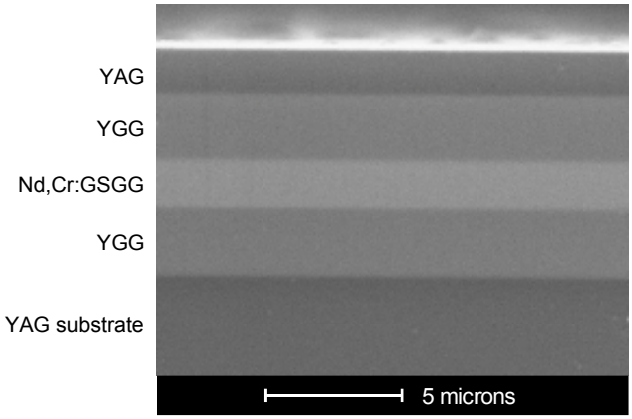


Figure 3